Aachen Institute for Advanced Study in Computational Engineering Science

Preprint: AICES-2009-10

11/March/2009

Reynolds Stress Model Implementation for Hypersonic Flow Simulations

A. Bosco, B. Reinartz and S. Müller

RWTH AACHEN UNIVERSITY

AICES

Financial support from the Deutsche Forschungsgemeinschaft (German Research Association) through grant GSC 111 is gratefully acknowledged.

List of AICES technical reports: http://www.aices.rwth-aachen.de/preprints

REYNOLDS STRESS MODEL IMPLEMENTATION FOR HYPERSONIC FLOW SIMULATIONS

Arianna Bosco, PhD student, AICES
Birgit U. Reinartz, Research Fellow, CATS
Siegfried Müller, Privatdozent, IGPM
RWTH University, 52056 Aachen, Germany

Abstract

The simulation of hypersonic flows presents some difficulties due to the interaction between boundary layers and shock waves and to the high total enthalpy. In order to achieve more accurate numerical results, with respect to physics, a Reynolds stress model (RSM) is being implemented in the QUADFLOW solver for unstructured grids. This model, developed and tested by Eisfeld, showed promising results on structured grids. It is a combination of two RSM: one that performs better near the wall and another able to achieve good results in the far field. The implementation consisted of writing new routines for the source terms and their derivatives as well as modifying old routines for the computation of viscous fluxes, boundary conditions and far field conditions. Some preliminary results on the flat plate are presented here. The friction coefficient for different turbulence models and for the analytical solutions (the laminar of Blasius and the turbulent of Schultz-Grunow) is compared and the grid convergence of the model is analyzed.

1 Introduction

The aerodynamic design of hypersonic inlets is a critical issue for the overall performance of an air breathing propulsion system. Two phenomena characterize the technological problems of the inlet: on the one hand, the interaction of strong shock waves with thick hypersonic boundary layers causes large separation zones that reduce the captured mass flow and thus the engine performance. On the other hand, the high total enthalpy of the flow leads to severe aerodynamic heating, further enhanced by turbulent heat fluxes.
Currently, most of the turbulent flows are studied through the mean of the Reynolds Averaged Navier-Stokes (RANS) method, where the averaged governing equations are solved for the mean variables. One of the main issue of the RANS approach is to model the terms, mainly the Reynolds stress tensor, that appear after the averaging process and describe the turbulent contribution to the mean flow.
In order to model them, eddy viscosity models are widely employed since they are easy to implement and computationally convenient. Nevertheless these models show difficulties to correctly predict flow phenomena like shock boundary layer interaction, which are of great interest for hypersonic flow.
One of the limits of eddy viscosity models is that turbulence is modeled as an isotropic quantity. This hypothesis is not suitable for hypersonic flows where the strongly anisotropic flow phenomena, taking place in the boundary layer, have a great influence on the overall flow. For this reason a differential Reynolds stress model (RSM) [2],[3] -the SSG/LRR-ω model- is being implemented into QUADFLOW [6] a parallel adaptive compressible flow solver which employs locally refined meshes with hanging nodes. The model chosen in this article has been developed by Eisfeld, who implemented it in the flow solver FLOWer for structured grids [8].
Until now the model has been implemented into QUADFLOW. The RSM is tested on a flat plate test case and the results are compared to those obtained with other turbulence models implemented in QUADFLOW, specifically the Spalart Allmaras and Menter Shear Stress Transport (SST) k-ω, as well as with results obtained with FLOWer using the same RSM. The choice of implementing a RSM in QUADFLOW is motivated by the promising results obtained by the same model with FLOWer solver especially for separated flows.
Later on the model will be employed for the simulation of the hypersonic double wedge shock-boundary layer interaction (Figure 1) and the results will be compared with those of other turbulence models present in QUADFLOW. In addition a further comparison is possible with the numerical and experimental results presented in ref.[1] .

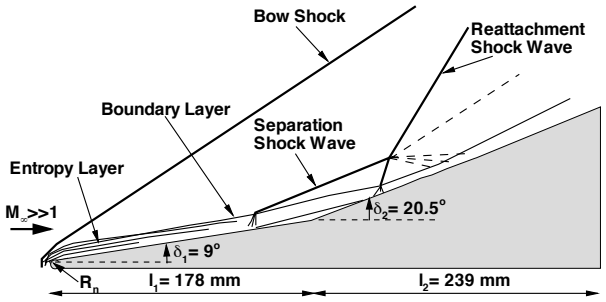

Figure 1: Shock / boundary layer interaction on a double wedge [1]

2 QUADFLOW Solver

QUADFLOW solves the Euler and Navier-Stokes equations around complex aerodynamic configurations. It uses a cell-centered finite volume method on locally refined grids. Mesh adaptation is based on multiscale analysis. The computational grids are represented by block-structured parametric B-Spline patches. For the computation of the convective flux, the flux-difference splitting HLLC Riemann solver by Batten and Leschziner is chosen. This method is capable of exactly preserving isolated shocks, contact and shear waves and it enforces the entropy condition in a way that no entropy correction of the primitive variables is employed.

For what concerns the computation of the viscous fluxes, the gradients of the variables at cell interfaces are determined using the divergence theorem. The computations presented here are steady state analyses so that time plays the role of an iteration parameter to achieve asymptotically stationary flow in the computation. The numerical methods employed are a Runge-Kutta fifth-order explicit scheme and a Backward Euler time integration for implicit treatment. In the QUADFLOW solver different turbulent models can be chosen. These are all RANS eddy viscosity models, in which the same proportionality between Reynolds stress tensor and the strain rate tensor as for the viscous stresses of a Newtonian fluid in laminar flow is considered. Even though these models are easy to implement and computationally convenient, they appear to be not suitable to simulate flow phenomena like shock boundary layer interaction in hypersonic flow. The models considered in this article and used to compare the results are the Spalart Allmaras model modified by Ashford and the Menter Shear Stress Transport (SST) k-ω model.

3 Reynolds Stress Models

Another type of RANS turbulence models are the differential Reynolds Stress Models where an equation is written and solved for each component of the symmetric Reynolds tensor defined as:

$$\bar{\rho}\tilde{R}_{ij} = \overline{\rho u_i'' u_j''} \tag{1}$$

where the superscript $\bar{}$ denotes the simple average and $\tilde{}$ the Favre (or mass) average and $'$ (which appears later on) and $''$define the corresponding fluctuations.

RSM is also referred to as second-order closure model. This means that the second order correlations for the fluctuating velocity components are computed while the higher correlations are modeled.

In order to obtain the equations describing the Reynolds stresses the first momentum of the Navier-Stokes equation is considered. This is done by multiplying the equation by a fluctuating velocity component and time averaging the product. If N is the operator that represents the Navier-Stokes equation, then we obtain the Reynolds Stress equation from [9]:

$$\overline{u_i'' N(\tilde{U}_j) + u_j'' N(\tilde{U}_i)} \quad . \tag{2}$$

After reorganizing the various terms, the final transport equations read as follows:

$$\frac{\partial}{\partial t}(\bar{\rho}\tilde{R}_{ij}) + \frac{\partial}{\partial x_k}(\bar{\rho}\tilde{U}_k\tilde{R}_{ij}) = \bar{\rho}P_{ij} + \bar{\rho}\Pi_{ij} - \bar{\rho}\epsilon_{ij} + \bar{\rho}D_{ij} + \bar{\rho}M_{ij} \quad . \tag{3}$$

The terms that appear at the right hand side of the equation represent the production, the redistribution, the destruction, the diffusion and the contribution of the turbulent mass flux, respectively.

Apart from the production term, which does not need modeling because it only depends on quantities for which an equation is solved,

$$\bar{\rho}P_{ij} = -\bar{\rho}\tilde{R}_{ik}\frac{\partial \tilde{U}_j}{\partial x_k} - \bar{\rho}\tilde{R}_{jk}\frac{\partial \tilde{U}_i}{\partial x_k} \quad , \tag{4}$$

the other terms, that is to say the re-distribution term

$$\bar{\rho}\Pi_{ij} = \overline{p'\left(\frac{\partial u_i''}{\partial x_j} + \frac{\partial u_j''}{\partial x_i}\right)} \quad , \tag{5}$$

the destruction term

$$\bar{\rho}\epsilon_{ij} = \overline{\tau_{ik}'\frac{\partial u_j''}{\partial x_k} + \tau_{jk}'\frac{\partial u_i''}{\partial x_k}} \quad , \tag{6}$$

the diffusion term

$$\bar{\rho}D_{ij} = \tag{7}$$

$$-\frac{\partial}{\partial x_k}[\overline{\rho u_i'' u_j'' u_k''} + (\overline{p' u_i''}\delta_{jk} + \overline{p' u_j''}\delta_{ik}) - (\overline{\tau_{ik}' u_j'' + t_{jk}' u_i''})]$$

and the contribution of the turbulent mass flux due to the compressibility effects

$$\bar{\rho}M_{ij} = \overline{u_i''}\left(\frac{\partial \bar{\tau}_{jk}}{\partial x_k} - \frac{\partial \bar{p}}{\partial x_j}\right) + \overline{u_j''}\left(\frac{\partial \bar{\tau}_{ik}}{\partial x_k} - \frac{\partial \bar{p}}{\partial x_i}\right) \tag{8}$$

need to be modeled. The way the different terms are modeled determines the particular type of Reynolds Stress Model.

3.1 Reynolds stress transport equation

The model chosen to be implemented in QUADFLOW is the SSG-LRR/ω turbulent model in which the Menter ω-equation has been used to provide the length scale [7]. This model has been developed by Eisfeld [2] and is the combination of the LRR model near the wall [4] and the SSG model [5] in the far field. The blending function of Menter has been employed to blend the coefficients of the two models.

The re-distribution term is modeled as follows

$$\begin{aligned}\bar{\rho}\Pi_{ij} = &-(C_1\bar{\rho}\epsilon + \frac{1}{2}C_1^*\bar{\rho}P_{kk})\tilde{b}_{ij} \\ &+C_2\bar{\rho}\epsilon(\tilde{b}_{ik}\tilde{b}_{kj} - \frac{1}{3}\tilde{b}_{mn}\tilde{b}_{mn}\delta_{ij}) \\ &+(C_3 - C_3^*\sqrt{II})\bar{\rho}\tilde{k}\tilde{S}_{ij}^* \\ &+C_4\bar{\rho}\tilde{k}(\tilde{b}_{ik}\tilde{S}_{jk} + \tilde{b}_{jk}\tilde{S}_{ik} - \frac{2}{3}\tilde{b}_{mn}\tilde{S}_{mn}\delta_{ij}) \\ &+C_5\bar{\rho}\tilde{k}(\tilde{b}_{ik}\tilde{W}_{jk} + \tilde{b}_{jk}\tilde{W}_{ik}) \quad ,\end{aligned} \tag{9}$$

where all the coefficients are obtained inserting the values in table (1) in the blending function (23) described below. In the above equation $\tilde{k}$ is the turbulent kinetic energy

$$\tilde{k} = \frac{\tilde{R}_{kk}}{2} \tag{10}$$

and ϵ is the specific dissipation

$$\epsilon = C_\mu \tilde{k}\omega \quad , \tag{11}$$

where C_μ is constant and equal to 0.09. The tensor appearing in equation (9) are the anisotropy tensor

$$\tilde{b}_{ij} = \frac{\tilde{R}_{ij}}{2\tilde{k}} - \frac{\delta_{ij}}{3} \quad , \tag{12}$$

and II its second invariant

$$II = \tilde{b}_{ij}\tilde{b}_{ij} \quad , \tag{13}$$

the strain rate tensor

$$\tilde{S}_{ij} = \frac{1}{2}\left(\frac{\partial \tilde{U}_i}{\partial x_j} + \frac{\partial \tilde{U}_j}{\partial x_i}\right) \quad , \tag{14}$$

the rotation tensor

$$\tilde{W}_{ij} = \frac{1}{2}\left(\frac{\partial \tilde{U}_i}{\partial x_j} - \frac{\partial \tilde{U}_j}{\partial x_i}\right) \tag{15}$$

and the traceless strain rate tensor $\tilde{S}_{ij}^*$.
The isotropic destruction term for both models reads:

$$\bar{\rho}\epsilon_{ij} = \frac{2}{3}C_\mu\bar{\rho}\tilde{k}\omega\delta_{ij} \quad . \tag{16}$$

For what concerns the diffusion term the generalized gradient diffusion model is choosen:

$$\bar{\rho}D_{ij} = \frac{\partial}{\partial x_k}\left[\left(\bar{\mu}\delta_{kl} + D^{(GGD)}\frac{\rho}{\omega}\tilde{R}_{kl}\right)\frac{\partial \tilde{R}_{ij}}{\partial x_l}\right]. \tag{17}$$

The value of the constant $D^{(GGD)}$ is computed through the equation:

$$D^{(GGD)} = F\sigma^* + (1-F)\frac{C_s}{C_\mu} \quad . \tag{18}$$

F is the blending equation in (23), σ^*= 0.5 and C_s=0.22.
Finally the term $\bar{\rho}M_{ij}$ is neglected.

The Menter ω-equation for RSM reads as follows:

$$\begin{aligned}&\frac{\partial}{\partial t}(\bar{\rho}\omega) + \frac{\partial}{\partial x_k}(\bar{\rho}\tilde{U}_k\omega) = \\ &\bar{\rho}P^\omega - \bar{\rho}D^\omega + \frac{\partial}{\partial x_k}\left[\left(\bar{\mu} + \sigma_\omega\frac{\bar{\rho}\tilde{k}}{\omega}\right)\frac{\partial \omega}{\partial x_k}\right] + \bar{\rho}C_D\end{aligned} \tag{19}$$

with the production term

$$\bar{\rho}P^\omega = -\alpha_\omega\frac{\omega}{k}\tilde{R}_{ik}\frac{\partial \tilde{U}_i}{\partial x_k} \quad , \tag{20}$$

the destruction term

$$\bar{\rho}D^\omega = \beta_\omega\bar{\rho}\omega^2 \tag{21}$$

and the cross-diffusion term

$$\bar{\rho}C_D = \sigma_d\frac{\bar{\rho}}{\omega}\max\left(\frac{\partial \tilde{\mathrm{k}}}{\partial \mathrm{x_k}}\frac{\partial \omega}{\partial \mathrm{x_k}}; 0\right) \quad . \tag{22}$$

The coefficients of the ω-equation as well as those of the Reynolds Stress are blended using the following function:

$$\phi = F\phi^{LRR} + (1-F)\phi^{SSG} \tag{23}$$

The coefficient for the ω-equation are listed in table (2).
The blending function of Menter is defined as:

	C_1	C_1^*	C_2	C_3	C_3^*	C_4	C_5
SSG	3.4	1.8	4.2	0.8	1.3	1.25	0.4
LRR	3.6	0	0	0.8	0	2.0	1.11

Table 1: Coefficients of SSG and LRR model for the re-distribution term [2]

	α_ω	β_ω	σ_ω	σ_d
SSG	0.44	0.0828	0.856	$2\sigma_\omega$
LRR	0.5556	0.75	0.5	0

Table 2: Coefficients for ω-equation [2]

$$F = \tanh(\zeta^4) \tag{24}$$

with

$$\zeta = \min\left[\max\left(\frac{\sqrt{\tilde{\mathrm{k}}}}{\mathrm{C}_\mu \omega \mathrm{d}}; \frac{500\bar{\mu}}{\bar{\rho}\omega \mathrm{d}^2}\right); \frac{4\sigma_\omega^{(\mathrm{SSG})}\bar{\rho}\tilde{\mathrm{k}}}{\bar{\rho}\mathrm{C}_\mathrm{D}^{(\mathrm{SSG})}\mathrm{d}^2}\right]. \tag{25}$$

3.2 Boundary conditions

As freestream conditions a unit Reynolds number (Re) of 3.5x10^6 and a Mach number (M) of 0.2 have been imposed. The incoming turbulence intensity (I) is chosen equal to 0.5%
At the subsonic inflow and outflow boundaries, characteristic boundary conditions are prescribed. Outgoing Riemann invariants are determined by quantities being extrapolated from the interior domain, while incoming Riemann invariants are set by free stream conditions. Symmetry boundary conditions are prescribed on the boundary part that precedes the flat plate leading edge. The flat plate is considered as a Navier-Stokes wall: at wall boundary cells, the coordinate location that is associated with the vector of unknowns is shifted from the cell centroid to the midpoint of the corresponding wall edge. For what concerns the turbulence variables the initial and far-field values are obtained through the following equations where the Reynolds stresses values are derived from the turbulent kinetic energy.

$$\tilde{k}_\infty = \frac{3}{2}(\mathrm{I}\cdot \mathrm{M}_\infty \cdot \mathrm{c}_\infty)^2 \quad \tilde{\mathrm{R}}_{\mathrm{ij}\infty} = \frac{2}{3}\tilde{\mathrm{k}}_\infty \tag{26}$$

$$\tilde{\omega}_\infty = \frac{\rho_\infty \cdot \tilde{k}_\infty \cdot \mathrm{Re}_\infty}{\mu_{t\infty}} \tag{27}$$

At the wall the Reynolds stresses are put to zero due to non slip condition. For the ω-equation the Menter approach is chosen with constant wall temperature.

4 Implementation

The implementation of the RSM into the QUADFLOW solver can be divided into basically five steps. First of all some modifications have been required to add an additional turbulence model with a different number of equations with respect to those already in there. The RSM is, in fact, a 7-equation turbulence model while the most common eddy viscosity models have one or two turbulence equations.
After that, the source terms have been implemented as well as their derivatives. These are employed both for the implicit time integration for the computation of the Jacobian matrix and for the explicit time integration, since the turbulent source terms are always treated implicitly.
As a third step, the viscous fluxes have been considered. On the one hand the viscous fluxes for the Reynolds stresses needed to be added to the solver. On the other hand the viscous fluxes of the momentum and energy equations needed to be modified by adding the contribution of the Reynolds Stress to the mean flow. In contrast to eddy viscosity models, these additional terms to the mean flow are not represented by the turbulent viscosity but by the components of the Reynolds stresses themselves. Furthermore, the derivatives of the viscous fluxes are needed for implicit time integration.
The last part of the work consisted of implementing the boundary conditions at solid walls, the far field conditions, the initial conditions and the non-dimensional form of the Reynolds Stress.
Some further routines have been modified to limit the values of the variables, to add the constants that appear in the model and to compute the turbulent viscosity from the model variables. For what concerns the computation of the convective fluxes, no further implementation has been required.

5 Flat Plate

As a first test case an incompressible flat plate test case is employed. The results obtained with the newly im-

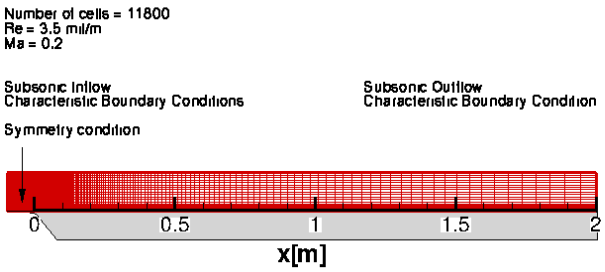

Figure 2: Computational grid for flat plate simulation

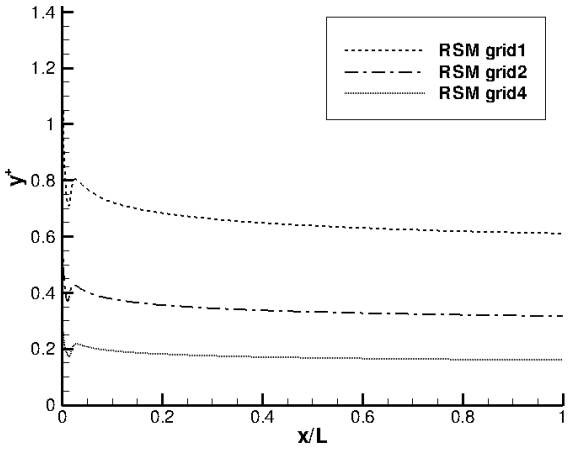

Figure 3: Non-dimensional distance of the first cell from the wall for different grids.

plemented RSM are compared to results obtained with QUADFLOW using Spalart Allmaras and Menter SST models as well as to results obtained with FLOWer using the SSG/LLR-ω model and to analytical results. The aim of this simulation is to show that the RSM can provide results in agreement with other turbulence models. The choice of a subsonic simulation is justified by the abundance of results and analytical solutions that can be employed for the comparison.

5.1 Problem description

For this simulation with the RSM in QUADFLOW three different computational grids have been employed. These are all structured grids with an increasing number of cells. The coarser grid (grid1) is presented in Figure 2. It consists of 11800 cells: 295 in the x-direction and 40 in the y-direction. The next grid (grid2) has a double number of grid cells and the finer grid (grid4) has four times the number of the grid cells of the coarser grid. Every grid is obtained by the previous one splitting every cells in half parallel to the x-direction. The results from Spalart Allmaras and Menter SST model are obtained using grid1.

5.2 Results

In Figure 3 the non-dimensional distance of the first cell from the wall is presented for the three grids used for the simulation on the flat plate. One can notice that this value is halved, as expected, passing from a grid to a finer one. Figure 4 shows the behavior of the friction coefficient for different turbulence models, on grid1, as well as the turbulent analytical solution of Schultz-Grunow and the laminar analytical solution of Blasius.

As one can notice, the Spalart Allmaras model follows the analytical solution quite closely apart from the values near the leading edge where the profile is closer to the laminar one.

Considering the Menter SST model, the friction coefficient, though close to the analytic value, is always under-predicted and there is a laminar region near the leading edge, though less pronounced than in the Spalart Allmaras simulation.

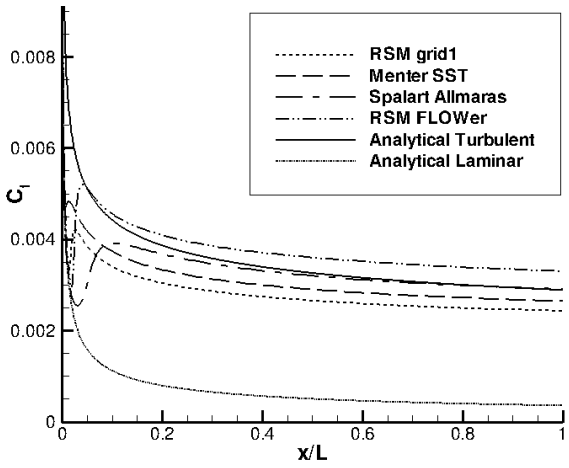

Figure 4: Comparison of friction coefficient for different turbulence models.

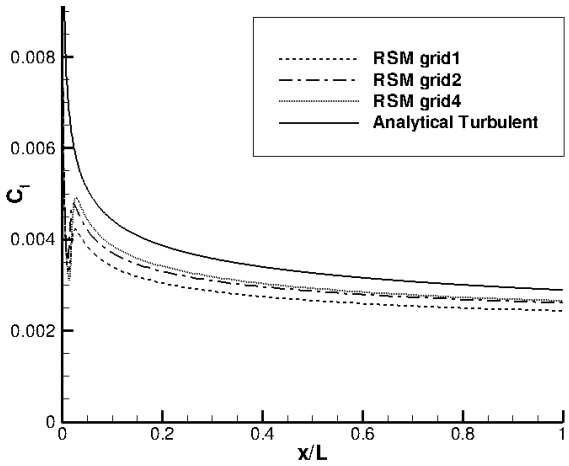

Figure 5: Comparison of friction coefficient obtained with RSM and different grids.

The result obtained with RSM in QUADFLOW shows a laminar behavior near the leading edge and then the friction coefficient increases but the values obtained always underestimate the analytical solution. The friction coefficient obtained with FLOWer is, on the contrary, larger than the exact one and this is probably due to the grid that is not fine enough to allow convergence.

The grid convergence for the RSM is analyzed in Figure 5 considering the friction coefficient. The refinement of the grid leads towards an improved solution, however the skin friction coefficient is still underpredicted for unknown reasons. Nevertheless, it is expected that the performance of the RSM will improve for compressible flow with strong pressure gradients.

6 Outlook

The implementation of the RSM in QUADFLOW solver is still under validation. After the encouraging results obtained on the flat plate test case the aim is to use the RSM model for the simulation of the hypersonic double wedge shock-boundary layer interaction.

References

[1] J. Ballmann B. Reinartz. Computation of Hypersonic Double Wedge Shock/Bondary Layer Interaction. *26th International Symposium of Shock Waves (ISSW 26)*, July 2007.

[2] B.Eisfeld. *Implementation of Reynolds stress models into the DLR-FLOWer code.* Internal DLR report IB 124-2004/31, december 2004.

[3] B.Eisfeld and O.Brodersen. Advanced Turbulence Modelling and Stress Analysis for the DLR-F6 Configuration. *AIAA Applied Aerodynamics Conference*, 2005-4727, 2005.

[4] G.J.Reece B.E.Launder and W.Rodi. Progress in the development of a Reynold-stress turbulence closure. *Journal of Fluid Mechanics*, 68:537–566, 1975.

[5] S.Sarkar C.G.Speziale and T.B.Gatski. Modelling the pressure-strain correlation of turbulence: an invariant dynamical system approach. *Journal of Fluid Mechanics*, 227:245–272, 1991.

[6] D.C.Wilcox. *Turbulence Modelling for CFD*. DCW Industries Inc., 1993.

[7] P.Lamby F.Bramkamp and S.Müller. An adaptive multiscale finite voulme solver for unsteady and steady state flow computations. *Journal of Computational Physics*, 197:460–490, 2004.

[8] F.R.Menter. Two-Equation Eddy-Viscosity Turbulence Models for Engineering Applications. *AIAA Journal*, 32(8):1598, 1605 1994.

[9] K.Becker N. Kroll, C.C.Rossow and F.Thiele. The MEGAFLOW Project. *Aerospace Science and Technology*, 4(4):223–237, 2000.